Long-range interactions in mammalian platelet aggregation
II. The role of platelet pseudopod number and length

Mony Frojmovic,* Kimberly Longmire,* and Theo G. M. van de Ven‡
*Department of Physiology, ‡The Pulp and Paper Research Institute of Canada, and ‡The Department of Chemistry, McGill University Montreal, Quebec, Canada

ABSTRACT In part 1, we reported that human (H) platelets, activated with high concentrations (10 μM) of adenosine diphosphate, aggregate under Brownian diffusion (nonstirred, platelet-rich plasma) with an apparent efficiency of collision (α_B) ~4 times and 8 times larger than observed, respectively, for canine (C) and rabbit (R) platelets. Further evaluations of parallel inhibition of α_B and shape change suggested a central role for platelet pseudopods in mediating the long-range interactions associated with the elevated α_B values. We found that >90% of all platelet contacts in the doublets and triplets formed were via at least one pseudopod. We therefore compared pseudopod number and length per platelet generated by ≈30 s post ADP activation in nonstirred PRP from human, canine, and rabbit donors, using phase-contrast, video-enhanced microscopy of fixed platelets. Theoretical calculations assessing the effects of pseudopod length and number on the collision frequency enhanced by an increased radius of a collision sphere supported the experimental observations that ≈3 or 4 pseudopods per human or canine platelet, and ≈5 or 6 pseudopods per rabbit platelet yield optimal α_B values, with the average pseudopod length: ≈3:2:1 for H/C/R, paralleling the α_B differences. After correcting for effects of pseudopods and platelet size on platelet diffusion and sedimentation, it still appeared that the small number of long pseudopods formed on human platelets could largely explain the unusually large α_B values. The quantitative discrepancies between theory and experiment do not appear related to time-dependent refractoriness within the <60 s of observation, but may be related to biochemical differences in dynamics and surface density of adhesive (sticky sites) present on the pseudopod surface.

INTRODUCTION

For blood flowing through blood vessels, the primary mode of transport of blood platelets to the vessel wall may be mediated by effects of red cells on radial displacement of platelets toward the vessel wall, as demonstrated with latex spheres of similar size as human platelets (1). However, other enhancements in platelet diffusion toward or effective collisions with blood cells or the vessel wall could arise from contributions of the nonspherical platelet, such as from motile pseudopods formed with platelet activation (2), particularly in low flow regimes associated, for example, with cardiovascular disease (1). It is widely recognized that pseudopods can facilitate cell to cell adhesive contacts by (*a*) minimizing electrostatic repulsions (3) and (*b*) providing a structural framework for intercellular membrane spreading for "stabilization" of adhesive contacts (4). In addition, it has been recognized that platelet shape change allowing aggregation of platelets in flow requires >1 pseudopod per platelet (5, 6) without any necessary change in main body shape (7, 8). However, no direct experimental nor theoretical treatments have appeared to date on the relation of platelet pseudopod size, number, and efficiency of aggregation.

The simplest approach to evaluating the magnitude of platelet diffusion which is in excess of that predicted for simple, spherical particles is to directly measure the rate of doublet and small multiplet formation of platelets. We observed in studies with human, dog, and rabbit platelets in part 1, applying Smoluchowski's theory, that unusually rapid aggregation occurs in ADP-activated platelet-rich plasma (PRP) suspensions stirred for <0.5 s to ensure efficient mixing of the activator without causing significant stir-induced aggregation. The apparent α_B values measured over the first 30–60 s post-ADP addition in these nonstirred PRP suspensions were <1.0, >1, and ≫1 for rabbit, dog, and human platelets, respectively. This was suggestive of long-range interactions mediated, for example, by surface projections or pseudopods operating to bring platelets together at considerably faster rates than predicted from diffusion of spherical particles (9). The nature of the unusually high α_B values observed for human platelets was first assessed by examining the sensitivity of no-stir vs. stir-associated aggregation to inhibition by selected inhibitors, which pointed to a central role for shape change. We then explored the differences in α_B between human, dog, and rabbit plate-

This work was presented in part at the XIIth International Congress of Hemostasis and Thrombosis, Tokyo, August, 1989.
Address reprint requests to Dr. Mony Frojmovic, Department of Physiology, McGill University, 3655 Drummond St., Rm. 1102, Montreal, Quebec, Canada, H3G 1Y6

lets by comparing platelet pseudopod number and size and the extent of pseudopod-mediated platelet contacts in the doublets which are primarily formed for 10 μM ADP in nonstirred suspensions for all three species. It was generally found that increasing pseudopod length paralleled the increasing α_B values measured at early times (<60 s) post-ADP addition in nonstirred suspensions, consistent with theoretical considerations presented here in detail. A model for the interspecies differences in α_B and for the deviations from theoretical predictions is presented in terms of the physical and expected biochemical properties of pseudopod membrane surfaces participating in platelet aggregate formation.

METHODOLOGY

Preparation of platelet-rich plasma

Human donors were healthy males and females between the ages of 19 and 45 yr, not on any medication, and informed consent was obtained. Mongrel dogs and New Zealand albino rabbits (males and females) weighed, respectively, 10–20 kg and 3–5 kg. Blood was collected from human, rabbit, and canine donors as previously described in part 1. In all cases, blood was collected directly into 3.8% sodium citrate (1:9 vol/vol blood), and PRP was prepared and maintained at 37°C and pH 7.4 as described previously (10).

Platelet aggregation kinetics

Platelet microaggregation (PA) was estimated from the percent decrease in the number of particles as in part 1 (11).

Unstirred, diffusion-dependent studies were performed using 10 μM ADP as described in part 1; PRP was mixed with ADP for 0.5 s, and then incubated for varying times with no stir out to 300 s. Stir-dependent PA studies were conducted with continuous stirring after ADP addition and fixation at 3 and 10 s (part 1). Time-dependent refractoriness of platelet aggregation was evaluated as previously reported (13) by comparing stir-dependent PA values (PA_3 and PA_{10}) as a function of varying incubation times after the above 0.5 s stir (Table 1). Aggregation was arrested and stabilized by addition of 5 vol of 0.8% glutaraldehyde (part 1).

Inhibitor studies

Inhibition studies were conducted for human PRP activated with 10 μM ADP using the combination of acetylsalicylic acid (ASA) and prostaglandin E^1 (PGE_1). The combination of concentrations blocking stir-associated secondary aggregation (TA-2), normally associated with the release reaction (12) was determined with the aggregometry device measuring light transmission (part 1). Thus, 0.4 ml of PRP was preincubated with 0.1–1 mM of ASA and 0.1–1.5 μM of PGE_1 for 1 min, followed by addition of 10 μM ADP to the stirred suspension. Effects of increasing concentrations of these inhibitors on the above microaggregation studies were then determined for PA_3 and PA_{10} for continuously stirred suspensions, and for PA measured over 10–300 s for diffusion-dependent aggregation, as previously reported (13, 14).

The initial rates of platelet shape change (V_s) and of platelet macroaggregation (V_a) detected by changes in light transmission after addition of the 10 μM ADP to stirred PRP (0.4 ml) in a Payton aggregometer were determined as in part 1, with % inhibition then determined as above (14).

Platelet pseudopod contact, number, and size in aggregation

A drop of the glutaraldehyde-fixed samples prepared for estimating PA in nonstirred human, rabbit, or canine PRP for post-ADP addition times of 0, 10, 60, and 300 s, was transferred into a Vaseline well formed on a glass slide; covered and sealed with a coverslip (application of a slight pressure) (2) and viewed on a videomonitor (ITC-Ikegami; Ikegami Tsushinki, Co., Ltd., Tokyo) using phase contrast microscopy (40 × objective, 1.25 × Optovar, Universal Research Microscope; Carl Zeiss,

TABLE 1 Refractoriness of human, rabbit, and canine platelets to ADP (10 μM)

Prestir ADP incubation time	Extent of refractoriness for*					
	PA_3			PA_{10}		
	Human	canine	Rabbit	Human	canine	Rabbit
(s)			%			
0	—	—	—	—	—	—
10	2 ± 2‡	27	0	2 ± 6	0	0
20	8 ± 7	40	0	2 ± 3	0	1 ± 1
30	21 ± 20	37	0	6 ± 5	0.5	1 ± 2
60	33 ± 20	31	39 ± 52	22 ± 13	0	18 ± 12
120	—	—	65 ± 46	—	—	38 ± 5
300	42 ± 15	43	98 ± 4	34 ± 11	0	65 ± 20
PA @ 0 time (no prestir)	52 ± 16 (8)§ (24–73)	67 (2)‖ (66–68)	18 ± 3 (3) (14–20)	75 ± 6 (7) (63–81)	74.5 (2) (74–75)	66 ± 5 (3) (61–71)

*Corrected for no stir PA contributions.
‡Mean ± SD.
§Number of donors evaluated shown in brackets.
‖These two animals were distinct from those studied for Tables 2 and 3.

Inc., New York) and a solid-state camera (Panasonic WVCD51; Montreal Video, Montreal, Canada).

Platelet contacts viewed in rotating doublets were classified as either (*a*) pseudopod to pseudopod contact or platelet main body surface to pseudopod contact and identified as those doublets which were capable of moving independently of each other (see Fig. 1); or (*b*) platelet main body to main body contact and differentiated as those doublets that rotated as a single entity. The platelet pseudopod number (N) and length (ℓ) were measured from pseudopods protruding from unaggregated platelet surfaces, as each platelet was viewed freely rotating. 20 platelets were randomly selected for determining N per platelet, with one pseudopod randomly selected from each platelet for measurement of ℓ. The length of the pseudopods was measured on the screen using a cursor that is part of the Image Analyzer 2 program (Coreco, Inc., Montreal, Canada) installed in an IBM Personal Computer. The base-to-tip length was measured in pixels, with 9.3 pixels = 1 μm, calibrated with a micrometer scale. Reproducibility of lengths was ±3 pixels = 0.32 μm. No diffraction rings were discernible on the pseudopods in contrast to rings previously reported for the main platelet body (15).

MATERIALS

Trisodium citrate (J. T. Baker Chemical Co., Phillipsburg, NJ) and ADP (Sigma Chemical Co., St. Louis, MO) were prepared as previously described (10). Hematall isotonic diluent, azide free (Fisher Scientific Co., Montreal, Canada), was used for diluting samples for counting. Glutaraldehyde was freshly prepared in plain Tyrode's (pH 7.4) from an 8% solution (EM arade; Polysciences, Inc., Warington, PA). ASA (Sigma Chemical Co.) was freshly dissolved in DMSO to make a 30-mM stock solution. PGE_1 (Sigma Chemical Co.), stored as a solid at −20°C, was freshly dissolved in plain Tyrode's buffer, pH = 7.4, to make a 98-μM stock solution. Final DMSO vehicle addition to PRP was <1.0% vol/vol.

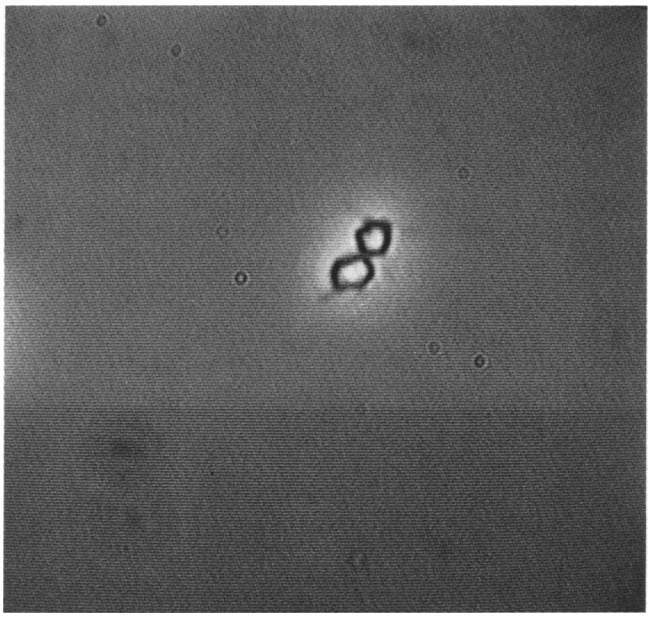

FIGURE 1 Two human platelets in a doublet linked via pseudopods each containing further numbers of extended pseudopods. Phase contrast micrograph of glutaraldehyde-fixed platelets after 30 s post ADP (10 μM) (no stir) using the phase-contrast microscope (40 × objective). The photograph was taken of a scene on the videomonitor (see Methods).

RESULTS

Relative inhibition of ADP-induced shape change and of stir- and nonstir-associated human platelet aggregation

In part 1, we reported that α_B values >1 for human platelet aggregation in nonstirred suspensions were observed only with high ADP and calcium ionophore A23187 concentrations. These concentrations are normally associated in stirred platelet suspensions with secondary aggregation and both α and dense granule release (12). Combinations of ASA and PGE_1 which inhibited ADP-induced shape change (SC) and aggregation were therefore evaluated, as these have been reported to optimally block even the partial granule secretion occurring with blood collection (16). The combination of ASA (100–1,000 μM) and PGE_1 (0.1–1.5 μM) was found to abolish stir-associated secondary aggregation, with associated release expected to be blocked (12), while causing major inhibition of stir-associated rate of macroaggregation (V_A) and variable inhibition of stir-associated microaggregation rate (PA_3) and extent (PA_{10}), as well as of rate of shape change (V_s), shown for three human donors in Table 2. Major inhibition of nonstir-associated aggregation, i.e., major reduction in α_B values, was observed for

TABLE 2 Differential inhibition of ADP-induced no-stir vs. stir-associated aggregation*

	Inhibitor		Stir % inhibition				No stir % inhibition		
Donor	ASA	$PGE_\perp$	V_b‡	PA_3	PA_{10}	V_s	α_B§	PA_{10-60}	PA_{300}
	μM								
1	*a* 100	1.5	69	6	15	0	1.6	6 ± 2	—
	b 1,000	1.5	78	24	17	45		85 ± 15	—
2	100	0.1	—‖	51	13	—	2.9	12 ± 12	24
3**	1,000	1.0	84	70	43	73	4.1	54 ± 10	81

*10 μM ADP was used as activator in all cases.

‡Note that in all cases secondary aggregation (TA2) has been effectively blocked.

§Values determined for 0–60 s without inhibitors for 10 μM ADP and no stir.

‖Not determined (—).

**$[ADP]_{1/2}$ for PA (<30 s) no stir and PA_3 stir was, respectively, 4.0 ± 0.3 and 1.0 μM.

experimental conditions, where in addition to the inhibition of stir-associated secondary aggregation (TA-2) and of rates of macroaggregation (V_A), major inhibition (45–73%) in rates of shape change was also observed. These experiments suggest that (*a*) platelet release is likely not associated with the observed α_B values, and (*b*) that shape change may play a major role in the kinetics of no stir-associated aggregation and the observed high α_B values.

Nature of pseudopods and platelet contacts in no stir-associated platelet aggregation

As reported in part 1 for human, dog, and rabbit platelets, ≥85% of all platelet aggregates formed with 10 μM ADP in nonstirred PRP were doublets, with the balance as triplets. Platelet to platelet contacts observed by direct microscopy were seen to consist essentially of pseudopod–pseudopod or pseudopod–main-body contacts (85–95% of all contacts), with <10–15% consisting of main-body to main-body contacts (Fig. 1). In light of such a major role for pseudopods, also suggested by the above inhibition studies, it was of interest to compare the number and length of pseudopods per platelet for human, canine, and rabbit platelets. It is seen from Table 3 that there are on average ~3–4 pseudopods per human or canine platelet and ~5–6 pseudopods per rabbit platelet at ~30 s after addition of 10 μM ADP. For human platelets, ~70% of these activated platelets are advanced discoechinocytes, i.e., discocytic with pseudopods, with the balance as spheroechinocytes (7); however, it is expected that discoechinocytes will be initially recruited as previously reported for stir-associated aggregation (8). It was unexpectedly observed that the average length of pseudopods on these ADP-activated platelets was ~3 times and 2 times greater, respectively, for human and canine platelets than for rabbit platelets (Table 3).

TABLE 3 Pseudopods on activated human, canine, and rabbit platelets: number per platelet and length

	Pseudopod	
	Number per platelet* N	Length‡ $\ell(\mu m)$
Human	3.5 ± 0.8 (2–5)‡	3.2 ± 0.8 (1.7–5.6)
Canine	4.0 ± 1.7 (2–7)	2.2 ± 0.8 (1.1–4.9)
Rabbit	5.5 ± 1.0 (4–7)	1.3 ± 0.3 (0.9–1.9)

*Measured for 20 singlet platelets in PRP for one donor each at 30 s post 10 μM ADP addition for "nonstirred" platelets, with 31%, 18%, and 12% aggregation, respectively, for H, C, and R donors.
‡Mean ± SD, with range of values shown in brackets.
§There is a highly significant difference between any combination of the two species: $p \leq 0.001$; 29 pseudopods per species analyzed.

Theory relating platelet aggregation in nonstirred suspensions to platelet size and shape

Smoluchowski's theory of coagulation

The aggregation of activated blood platelets is complicated by the fact that the platelets have a complex shape. When activated, the plate-like shape of platelets is changed into a less oblate shape from which several pseudopods are protruding. The length of the pseudopods can vary from a fraction of the platelet size to a length well exceeding the platelet length.

The problem of aggregation of spherical particles was considered first by Smoluchowski (17), who neglected in his theory the presence of colloidal interaction forces between the particles and the change in hydrodynamic resistance when the spheres approach. His theory works well when the only colloidal forces are attractive van der Waals dispersion forces, which approximately cancel the increased hydrodynamic drag. Smoluchowski's result for the rate at which spheres collide with a reference sphere in the fluid is

$$J_{SM} = 16\pi nDa = \frac{8}{3} n \frac{kT}{\mu}. \quad (1)$$

Here J_{SM} is the number of spheres colliding with the reference sphere per second, n is the number of spheres per unit volume, D is the diffusion constant of a sphere, a its radius, k is the Boltzmann constant, T the absolute temperature, and μ the viscosity of the medium. The last equality in Eq. 1 is derived from the Stokes-Einstein relation

$$Df = kT, \quad (2)$$

f being the friction coefficient which for a sphere equals $6\pi\mu a$.

Often the rate J_{SM} predicted by Smoluchowski is taken as a reference rate and the actual rate is expressed as

$$J = \alpha_{BM} J_{SM}, \quad (3)$$

where α_{BM} is the collision efficiency for Brownian motion-induced aggregation. Because J_{SM} is a somewhat arbitrary reference flux, α_{BM} can take on any value between 0 and ∞. For colloidal spheres subjected to electrostatic and van der Waals forces, α_{BM} can be calculated theoretically (9).

Because Eq. 1 predicts that J_{SM} is independent of particle size or shape, one might think that it could also be applied to particles of more complex shapes, such as, e.g.,

blood platelets. However, in Eq. 1, the product Da (which for spheres is independent of a) arises from Fick's first law of diffusion:

$$J_{SM} = 4\pi R^2 D(dn/dr)_R, \tag{4}$$

where R is the radius of the collision sphere (of radius $2a$) and $(dn/dr)_R = 2N_0/R$, N_0 being the concentration of platelets in the bulk. For activated platelets both R and D are different from the values for spheres and the product will no longer be independent of size and shape. To investigate this in more detail, we need estimates of the diffusion constant of platelets and the radius of their collision cross-sections.

Diffusion constant of activated platelets

The shape of an activated platelet can be thought of as an oblate spheroid from which several spikes are protruding. As a first approximation we will consider the activated platelet to be a sphere of radius a, from which N cylindrical spikes (pseudopods) are protruding of length ℓ and cross-sectional radius (of the spikes) s. The diffusion constant of such an object can be estimated by comparing it with a composite sphere, consisting of a solid sphere surrounded by a porous shell. Measurements of friction coefficient of hairy spheres are found to be in excellent agreement with this model (18). The results are expressed in the parameters α and β, where $\alpha = a/k$ and $\beta = b/k$, a being the radius of the solid nucleus and b of the composite sphere ($b = a + \ell$), k is the permeability of the shell, related to its volume fraction c by

$$k = -\frac{s^2}{8c}\left(lnc + \frac{1 - c^2}{1 + c^2}\right). \tag{5}$$

The theory (18) provides a somewhat complex relation $f(\alpha, \beta)$ between the friction coefficient f of the composite sphere and α and β. The volume fraction c can be found from

$$c = \frac{\pi s^2 \ell N}{4/3\pi(b^3 - a^3)}. \tag{6}$$

Hence, from the values of a, ℓ, s, and N, we can determine c and k and thus α and β and subsequently from the relation $f(\alpha, \beta)$ we can obtain f. The diffusion constant D then follows from Eq. 2. E.g., assuming $a = 1.2\ \mu m$, $\ell = 3.2\ \mu m$, $s = 0.1\ \mu m$, and $N = 4$ yields $c = 1.15 \cdot 10^{-3}$, $k = 6.3\ \mu m^2$, $\alpha = 0.48$, $\beta = 1.76$ and $f = 0.45 f_b$, f_b being the friction coefficient of a solid sphere of radius b. It follows from Eq. 2 that $D \simeq (a/0.45b)D_0 \simeq 0.6\ D_0$, D_0 being the diffusion constant of the sphere without the spikes (of radius a). It follows that in this case the presence of pseudopods decreases the diffusion constant by ~40%. It should be noted that in the absence of pseudopods the diffusion constant of a nonactivated platelet is smaller than that of an equivalent sphere (because of its nonspherical shape), but this will little affect the ratio D/D_0.

Radius of collision sphere of activated platelets

For activated platelets, the concept of a collision sphere becomes ill-defined because two platelets can be either in contact or not at a given distance, depending on whether or not the pseudopods make contact or simply interdigitate. Schematically the approach of two platelets is shown in Fig. 2.

If one assumes that two platelets come into effective contact when a pseudopod of an approaching platelet penetrates a distance d in the "porous shell" layer of the reference platelet, then the radius of the collision cross-section equals

$$R = 2a + 2\ell - d. \tag{7}$$

An estimate of d can be made by considering both the rotational and translational motion of the platelets and assuming that two platelets aggregate when two pseudopods make contact. Suppose a pseudopod has penetrated a distance d into the influence sphere of a reference platelet. What is the probability that the pseudopod makes contact with a pseudopod of the reference platelet before it diffuses out of the influence sphere? On average it takes a time

$$t_{trans} \sim d^2/2D \tag{8}$$

to diffuse out of the influence sphere of the reference platelet. During that time the reference platelet is rotating due to rotary Brownian motion and, if the particle rotates sufficiently, one of its pseudopods will make contact with one of the pseudopods of the approaching platelet before it can translate away. On average, the

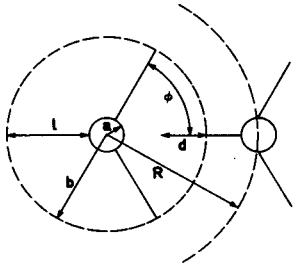

FIGURE 2 Schematics of two activated platelets approaching each other ($N = 3$).

angle ϕ between a pseudopod of the reference platelet and the projection of the nearest pseudopod of the approaching platelet will be $\phi \sim \pi/N$ (see Fig. 2). An estimate of d can be made by equating t_{trans} with t_{rot}, with t_{rot} given by

$$t_{rot} = \phi^2/2D_r, \tag{9}$$

D_r being the rotary diffusion constant, which for spheres equals $(3/4a^2)D$. Equating Eq. 8 with Eq. 9 yields for the penetration distance d

$$\frac{d}{a} \simeq \frac{4\pi}{3N}. \tag{10}$$

By combining Eqs. 7 and 10 it can be seen that the radius of the collision cross-section can be approximated as

$$\frac{R}{2a} \simeq 1 + \frac{\ell}{a} - \frac{2\pi}{3N}. \tag{11}$$

So far we have assumed that the platelets were spherical. Approximating their shape by an oblate spheroid of axis ratio $r_p = a_2/a_1$ ($r_p < 1$), it follows from Eq. 4 that R must be replaced by

$$R \simeq 2a_1a_2\,(\overline{2/r})_R.$$

However, because

$$\frac{\overline{2}}{r} \simeq \frac{1}{2}\left(\frac{2}{2a_1} + \frac{2}{2a_2}\right) = \frac{1}{2}\left(\frac{a_1 + a_2}{a_1 \cdot a_2}\right),$$

we conclude that $R \simeq a_1 + a_2 \simeq 2a_{eff}$, a_{eff} being the equivalent radius of the spheroid. It follows that Eq. 11 is also valid for spheroidal particles, provided a $\simeq$ $1/2\,(a_1 + a_2)$. This condition is satisfied for the different mammalian unactivated discocytes (Table 4) as well as for spheres ($a_1 = a_2$) and intermediate activated forms (6, 7).

TABLE 4 Size and shape of platelets

	Nonactivated platelets			
	Length	Width	Volume	Effective radius§
	(μM)	(μM)	(μM^3)	(μM)
Human*	3.6	0.9	4–8	1.2
Canine‡	3.6	0.9	4–8	1.2
Rabbit*	3.2	0.6	1–6	0.9

*Data previously reported for two human and four rabbit donors (15).
‡Data set to that for human platelets as mean electronic volumes have been reported as identical (21) and our analysis of one dog's PRP gave similar results: length 4.3 μm, width 0.9 μm, calculated volume 9 μm^3, and effective radius 1.29 μM.
§Determined for the volume of an equivalent sphere.

Collision efficiency of activated platelets

From the ratio D/D_0, and Eqs. 3 and 11, it follows that the collision efficiency for Brownian motion induced coagulation of activated platelets equals:

$$\alpha_{BM} \simeq \frac{D}{D_0}\left(1 + \frac{\ell}{a} - \frac{2\pi}{3N}\right). \tag{12}$$

The various terms in Eq. (12) all have a well-defined physical meaning. The term D/D_0 lowers the efficiency because of the decrease in Brownian motion. The first term in brackets is the efficiency of platelets without pseudopods, the second term increases the efficiency because of the presence of pseudopods, and the last term reduces it because pseudopods can diffuse out of the influence sphere of neighboring platelets before being captured. Because the relation $\phi \sim \pi/N$ is only expected to hold for a sufficient number of pseudopods, Eq. 12 can be expected to hold when $N > 2$.

Predictions of collision efficiencies as a function of the number of pseudopods are shown in Fig. 3.

It can be seen that for human platelets the efficiency is maximum (~200%) when $N = 3$ or 4. The decrease for large N is due to the fact that for a large number of pseudopods the particle starts to behave as a solid sphere of radius b and thus $\alpha_{BM} \rightarrow 1$ as $N \rightarrow \infty$. It follows that the formation of more than four pseudopods per platelet has no advantage in promoting aggregation. The reason is that the decrease in D/D_0 becomes more important than the increase in R. For canine and rabbit platelets, the maximum occurs near four and six pseudopods, respectively, and the maximum is much less pronounced.

Effects of sedimentation of platelets

Because not all platelets have exactly the same size and density, platelets will sediment with various sedimentation velocities. The difference in velocity can cause platelets to collide resulting in aggregation.

The number of particles sedimenting with velocity u_2 colliding with a reference particle sedimenting with

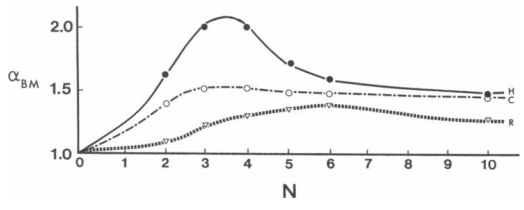

FIGURE 3 Predicted collision efficiencies as a function of the number of pseudopods for activated platelets. Human: $a = 1.2$ μm, $\ell = 3.2$ μm, $s = 0.1$ μm; Canine: $a = 1.2$ μm, $\ell = 2.2$ μm, $s = 0.1$ μm; Rabbit: $a = 0.9$ μm, $\ell = 1.3$ μm, $s = 0.1$ μm (taken from Tables 3 and 4).

velocity u_1 equals

$$J_{sed} = n\Delta u \pi R^2, \tag{13}$$

where n is the number of particles with velocity u_2, $\Delta u = u_2 - u_1$ and R is the radius of the collision cross-section, given by Eq. 7, but with d estimated as

$$d \simeq \frac{\Delta u \pi^2}{2N^2 D_r} \simeq \frac{4\pi^3 \mu a \Delta u}{N^2 kT}. \tag{14}$$

Each particle settles with a velocity determined by

$$mg = fu, \tag{15}$$

where g is the gravitational acceleration constant and m and f the mass and friction coefficients of the platelet. Hence

$$\Delta u = g\left[\left(\frac{4}{3}\pi a_2^3 + N_2 \pi s_2^2 l_2\right)\frac{\Delta\rho_2}{f_2} - \left(\frac{4}{3}\pi a_1^3 + N_1 \pi s_1^2 I_1\right)\frac{\Delta\rho_1}{f_1}\right]. \tag{16}$$

The subscripts 1 and 2 refer to the reference and approaching platelet, respectively. $\Delta\rho$ is the density difference between particle and fluid. The ratio of aggregation rates due to sedimentation and Brownian motion equals

$$\sigma = \frac{J_{sed}}{J_{BM}} = \frac{R\Delta u}{8D} \simeq \frac{6\pi\mu a^2 \Delta u}{kT}. \tag{17}$$

For human platelets, taking $a_2 = 1.3$ μm, $a_1 = 1.1$ μm, $\Delta\rho_2$ 30 kg/m^3, and $\Delta\rho_1$ 10 kg/m^3, results in values of Δu of ~50 nm/s, and values of σ in the range 0.1–0.3. It follows that aggregation due to sedimentation is less important than aggregation due to Brownian motion. When Brownian motion and sedimentation are both present, the coagulation rate is, when $\sigma \ll 1$, given (19), by

$$J = J_{BM}(1 + \alpha_{BM}\sigma). \tag{18}$$

It follows, if one defines an effective collision efficiency α_{eff} by $J = \alpha_{eff} J_{SM}$, that

$$\alpha_{eff} = \alpha_{BM}(1 + \alpha_{BM}\sigma). \tag{19}$$

Comparison between theory and experiments

An approximately inverse relationship was observed between the number of pseudopods per activated platelet (N) and the average length of pseudopods (ℓ) for human, canine, and rabbit platelets, i.e., rabbit platelets have the largest number of much shorter pseudopods per platelet than seen for canine or human activated platelets (Table 3). Average pseudopod lengths (ℓ) and equivalent sphere radii (Table 4) were used in calculating the collision efficiencies for Brownian motion, α_{BM}, for platelets from these three species (Fig. 3), as a function of N. These predicted α_{BM} values were found to have maximal values for N in the range actually observed experimentally (compare Fig. 3 and Table 3).

Using the average values of N and l in Table 1, we calculated the average values of the relative contributions of sedimentation to Brownian motion (σ), and the resultant effective collision efficiency (α_{eff}). These are presented in Table 5 and compared with experimentally observed values (α_{exp}) derived from the data presented in part 1.

It can be seen that the predictions and experiments agree within one standard deviation, although for rabbit platelets the mean experimental value is ~55% of the theoretical one. For human platelets the error in the experiments is rather large, possibly reflecting the difficulty in measuring initial aggregation rates. The theory applies to two platelet interactions only, not to the subsequent growth of aggregates. Table 5 shows that the decrease in diffusion constant (due to the presence of pseudopods) is more than offset by the increase in the radius of the collision cross-section.

DISCUSSION

In part 1, we found that the apparent efficiency of Brownian diffusion controlled aggregation (α_B) of platelets activated with high ADP concentrations varied as ~8:2:1 for human ≫ canine > rabbit platelets. We initially compared human and rabbit platelets, whose mean size differ by twofold (15), and then included canine platelets which are of identical size as human platelets (20) but which showed α_B values more comparable to that seen for rabbit platelets. Thus, α_B did not appear to depend on platelet volume. The most likely model for these large α_B values observed in part 1 appeared to be one based on long-range interactions associated with pseudopod production distinct for each of these species.

TABLE 5 Comparison between predicted and observed collision efficiencies

	D/D_o	$R/2a$	α_{BM}	σ	α_{eff}*	α_{exp}‡
Human	0.60	3.3	2.0	0.3	3.2 ± 0.7	8 ± 5
Canine	0.65	2.3	1.5	0.3	2.2 ± 0.6	2.1 ± 0.7
Rabbit	0.67	2.1	1.4	0.1	1.6 ± 0.3	0.9 ± 0.4

*Errors estimated from variations in number and length of pseudopods and uncertainty in pseudopod thickness. Other entries are average values. α_{eff} calculated from Eq. 19.
‡$\alpha_{exp} = \alpha_B$ values reported in part 1.

This was consistent with our observations in this report that a major reduction of α_B values for ADP-activated human platelets was only observed at concentrations of inhibitors causing parallel major inhibition of platelet shape change (ASA/PGE_1 in Table 2).

We examined experimentally and theoretically the relationship between platelet pseudopod number and size vs. α_B values obtained for human, rabbit, and canine platelets. We found surprisingly good correlations between our theoretical predictions and experimental observations. Thus, the average maximal number of pseudopods per platelet (N) present ~30 s after platelet activation with 10 μM ADP appears characteristic for each species evaluated, with only three to six pseudopods per platelet required to yield maximal predicted collision efficiencies (α_{BM} in Fig. 2), with greater N actually predicted to lower α_{BM}. The predicted optimal values of $N \sim 3$–4 for human and canine platelets, and ~6 for rabbit platelets, were experimentally observed (Table 3). These results are consistent with our observations that ≥85% of all platelet contacts in doublets or triplets formed in diffusion-controlled aggregation for all three species were via one or more pseudopods, directly visualized by microscopy. Such a central role for pseudopods as an absolute prerequisite for platelet to platelet contacts has been previously reported for continuously stirred platelet suspensions for ADP or adrenaline as activator, where ≥1–2 pseudopods per platelet on the surface even in the absence of main body shape change, appeared necessary for microaggregation (5, 8). Thus, 10 μM ADP-activated human PRP showed >85% of all doublets joined by at least one pseudopod whether ~30% of all platelets formed doublets by ~20–30 s of no stir or by ~2 s of continuous stir.

In stirred suspensions, rapid rotation of platelets abolishes the advantages conferred by the distinct platelet number and length of pseudopods on human platelets vs. canine or rabbit platelets, as no differences in continuously stir-associated rates of microaggregation were observed for these three species (part 1). However, the effect of pseudopods on the radius of the collision cross-section of human platelets in Brownian diffusion-associated aggregation vs. canine and rabbit platelets has been predicted to yield relative α_B values, corrected for differences in diffusion and sedimentation, of the order of 4:2:1 (see α_{eff} in Table 5). In particular, however, α_{eff} predicted for human platelets appears up to ~50% smaller than experimentally observed. This could arise from an underestimation of effective pseudopod lengths (ℓ) associated with our studies of glutaraldehyde-fixed cells, because it has been reported that human platelet pseudopods can dynamically extend and retract by up to 50% of their time-averaged length (2). Possible error in pseudopod length, ℓ, due to our measurement of only unaggregated platelets, was shown to be negligible. We compared ℓ for human PRP activated with 10 μM ADP for 30 s (no stir) at platelet counts of 335,000 μl^{-1} and diluted to 36,000 μl^{-1} respectively, yielding microaggregation of 38 ± 1% and 2 ± 2%. Mean ℓ values for the partially aggregated and nonaggregated PRP were identical, respectively, 3.1 ± 0.4 μm and 3.1 ± 0.6 μm.

Given the lower α_B observed values for rabbit platelets than theoretically predicted (Table 5), and given the decrease in α_B toward lower and comparable values (~0.5) for all three species' platelets when analyzing the aggregation data for nonstirred platelet suspensions over longer times after ADP addition (part 1), the possible contribution of time-dependent loss of platelet functional response to 10 μM ADP was evaluated for stirred platelets from all three species (Table 1). As previously reported for human PRP studied with 2 μM ADP (13), ≥95% of human platelets remained aggregable when stirred after <30 s preincubation times with ADP (PA_{10} in Table 1), with only minor inhibition of rates of aggregation (PA_3 values in Table 1). This was also observed for canine and rabbit platelets, suggesting that refractoriness over the early times of observation (<30 s) is not a significant factor in explaining the experimental differences in α_B values observed at these early times. In addition, time-dependent decay in α_B at post-ADP times of >60 s can only partially be explained by the stir-dependent measurements, with the highly variable results at times >60 s (Table 1) not reflected in the α_B measurements.

Our observations on the apparent dependence of α_B on pseudopod length (ℓ) for activated platelets from three different species (Table 5) raise the possibility that the large decreases in α_B seen for human platelets with (*a*) increasing postactivation time (Fig. 4 in part 1) or with (*b*) decreasing ADP activator concentration (Table 4 in part 1), may be related to corresponding changes in pseudopod length (ℓ). However, the above changes in α_B were not paralleled by any significant changes in ℓ as determined with one human donor's platelets: (*a*) ℓ = 2.6 ± 1.0 μm and 2.8 ± 1.0 μm for 10 μM ADP activation observed at 30 s and 5 min, respectively, and (*b*) ℓ = 2.7 ± 1.0 μm and 3.1 ± 0.9 μm for 5 μM and 1 μM ADP activation, respectively, measured at 30 s.

A distinct time-dependent mechanism may exist for refractoriness of unstirred platelets centered, e.g., on a time-dependent loss in stickiness of one or more pseudopods, e.g., redistribution of sticky sites toward the pseudopod base or platelet main body. Such a pseudopod-dependent refractoriness would not be expected to be as important in stir-associated aggregation where platelet rotary diffusion is slow compared with very rapid flow-associated platelet collisions. It is widely accepted that the sticky sites on activated platelet surfaces which mediate platelet aggregation usually consist of fibrinogen specifi-

cally bound to its integrin receptor, glycoprotein IIb-IIIa (21–23.). The ability of these fibrinogen-occupied membrane surface receptors to move together into surface clusters is well documented (21, 22). Intrinsic species-dependent differences in the generation of sticky sites on activated platelet pseudopods could also explain the differences in α_B observed at early times from values predicted theoretically (Table 5), e.g., human platelet pseudopods may have greater numbers of fibrinogen receptors (sticky sites) per unit area of membrane than do rabbit platelet pseudopods. This could result in shorter interpenetration distances required for two rabbit platelets, i.e., shorter, effective radius of collision and correspondingly smaller values of α_{BM} than predicted from maximal pseudopod lengths. These aspects of sticky properties of pseudopods is being evaluated with immunocytochemical electron microscopy (21, 22).

The requirement of high ADP concentrations for achieving maximal α_B values much in excess of that required for maximal rates of stir-associated aggregation (part 1) is also consistent with the need to form maximal numbers of fibrinogen sticky sites on platelet pseudopods (23). A minor role is expected for the release of adhesive proteins such as thrombospondin or new receptors for fibrinogen (23), because (*a*) minor release is expected in our experimental conditions where only doublets and triplets are formed (6) and (*b*) α_B was not significantly affected when combinations of inhibitors were used at concentrations blocking stir-associated secondary aggregation/release (Table 2) (12) and reported to block even the minor release occurring with blood collection (16). Thus, neither the endoperoxide pathway, irreversibly blocked by >100 μM ASA (12), nor dense granule release, blocked by ASA/PGE_1 (16), appear necessary for the apparent long-range interactions associated with the high α_B values.

It is expected that the physical and biochemical properties of platelet pseudopods may play a major role in regulating adhesive events with other blood cells and surfaces occurring in hemostasis and thrombosis in a variety of flow regimes and clinical conditions. For example, the effects of increased numbers of circulating platelets with pseudopods in thromboembolic complications, as recently reported for patients with coronary and cerebral artery disease (24), remain to be determined.

We appreciate the technical assistance of Ms. J. Wylie, Mr. T. Wong, and Ms. A. Jenkins.

This work was supported by funds from the Medical Research Council of Canada and the Quebec Heart Foundation.

Received for publication 18 September 1989 and in final form 19 March 1990.

REFERENCES

1. Karino, T., and H. L. Goldsmith. 1987. Rheological factors in thrombosis and hemostasis. *In* Hemostasis and Thrombosis 2nd ed. A. L. Bloom and D. P. Thomas, editors. Churchill Livingstone, London. 739–755.
2. Allen, R. D., L. R. Zacharski, S. T. Widirstky, R. Rosenstein, L. M. Zaitlan, and D. R. Burgess. 1979. Transformation and motility of human platelets: details of the shape change and release reaction observed by optical and electron microscopy. *J. Cell Biol.* 83:126–142.
3. Weiss, L. 1964. Cellular locomotive pressure in relation to initial cell contacts. *J. Theor. Biol.* 6:275–281.
4. Marsh, S. A., and G. E. Jones. 1982. Microspike function in cell aggregation. *Eur. J. Cell Biol.* 282:278–280.
5. Oliver, J. A., and R. M. Albrecht. 1987. Colloidal gold labelling of fibrinogen receptors in epinephrine- and ADP-activated platelet suspensions. *Scan. Elec. Micros.* 1:745–756.
6. Frojmovic, M. M., and J. G. Milton. 1982. Human platelet size, shape, and related functions in health and disease. *Physiol. Rev.* 62:185–261.
7. Frojmovic, M. M., and J. G. Milton. 1983. Physical, chemical, and functional changes following platelet activation in normal and "giant" platelets. *Blood Cells.* 9:359–382.
8. Milton, J. G., and M. M. Frojmovic. 1984. Adrenaline and adenosine diphosphate-induced platelet aggregation require shape change. *J. Lab. Clin. Med.* 104:805–815.
9. van de Ven, T. G., and S. G. Mason. 1977. The microrheology of colloidal dispersions. VIII. Effect of shear on perikinetic doublet formation. *Colloid & Polym. Sci.* 255:794–804.
10. Tang, S. S., and M. M. Frojmovic. 1980. The effects of pCO_2 and pH on platelet shape change and aggregation for human and rabbit platelet-rich plasma. *Thromb. Res.* 10:135–145.
11. Frojmovic, M. M., J. G. Milton, and A. Gear. 1989. Platelet aggregation measured *in vitro* by microscopic and electronic particle counting. *Methods Enzymol.* 169:134–149.
12. Mills, D. C. B. 1982. The mechanism of action of antiplatelet drugs. *In* Hemostasis and Thrombosis. R. W. Colman, J. Hirsh, V. J. Marder, and E. W. Salzman, editors. J. B. Lippincott Co., Philadelphia. 1058–1067.
13. Frojmovic, M. M., J. G. Milton, and A. Duchastel. 1983. Microscopic measurements of platelet aggregation reveal a low ADP-dependent process distinct from turbidimetrically measured aggregation. *J. Lab. Clin. Med.* 101:964–976.
14. Pedvis, L., T. Wong, and M. M. Frojmovic. 1988. Differential inhibition of the platelet activation sequence: shape change, micro- and macro-aggregation, by a stable prostacyclin analogue (Iloprost). *Thombos. Haemostasis.* 59:323–328.
15. Frojmovic, M. M., and R. Panjwani. 1979. Geometry of normal mammalian platelets by quantitative microscopic studies. *Biophys. J.* 16:1071–1089.
16. Files, J. C., T. W. Maples, E. K. Yee, J. L. Ritchie, and L. A. Harker. 1981. Studies of human platelet α granule release in vivo. *Blood.* 58:607–618.
17. Smoluchowski, M. V. 1917. Versuch einer mathematischen Theorie der Koagulationskinetic Kolloider Losungen. *Z. Phys. Chem.* 92:129–168.
18. Masliyah, J. H., G. Neale, K. Malysa, and T. G. M. van de Ven. 1987. Creeping flow over a composite sphere: solid core with porous shell. *Chem. Eng. Sci.* 42:245–253.

19. Melik, D. H., and H. S. Fogler. 1984. Effect of gravity on Brownian motion. *J. Colloid Interface Sci.* 101:84–97.

20. Nakeff, A., and M. Ingram. 1970. Platelet count: volume relationships in four mammalian species. *J. Appl. Physiol.* 28:530–534.

21. Asch, A. S., L. L. K. Leung, M. J. Polley, and R. L. Nachman. Platelet membrane topography: colocalization of thrombospondin and fibrinogen with the glycoprotein II_b-III_a complex. *Blood.* 66:926–934.

22. Loftus, J. C., and R. M. Albrecht. 1984. Redistribution of the fibrinogen receptor of human platelets after surface activation. *J. Cell. Biol.* 99:822–829.

23. Nurden, A. T. 1987. Platelet membrane glycoproteins and their clinical aspects. *In* Thrombosis and Haemostasis. M. Verstraete, J. Vermylen, R. Lijnen, and J. Arnout. Leuven University Press, Belgium. 93–125.

24. Milton, J. G., and M. M. Frojmovic. 1987. Unusual properties of platelet shape in coronary and cerebral artery disease. *Thromb. Res.* 47:511–533.